Available online at BCREC website: https://bcrec.id

Bulletin of Chemical Reaction Engineering & Catalysis, 16 (2) 2021, 293-301

Research Article

Fe-doped TiO_2/Kaolinite as an Antibacterial Photocatalyst under Visible Light Irradiation

A.B. Aritonang[1,*)], E. Pratiwi[1], W. Warsidah[2], S.I. Nurdiansyah[2], R. Risko[2]

[1]*Department of Chemistry, Faculty of Mathematics and Natural Science, Tanjungpura University, Pontianak, 78124, Indonesia.*

[2]*Department of Marine, Faculty of Mathematics and Natural Science, Tanjungpura University, Pontianak, 78124, Indonesia.*

Received: 8th February 2021; Revised: 1st April 2021; Accepted: 2nd April 2021
Available online: 7th April 2021; Published regularly: June 2021

Abstract

In this work, undoped and Fe-doped TiO_2 immobilized on kaolinite surface was successfully synthesized by sol-gel method with various Fe concentrations (0.05, 0.125, and 0.25 wt%). The effects of Fe doping into TiO_2 lattice were thoroughly investigated by a diffuse reflectance UV-visible (DRS) spectroscopy, Fourier Transform Infrared (FTIR) spectroscopy, and X-ray diffraction (XRD). The optical band gap of undoped and Fe-doped TiO_2/kaolinite is red shifted with respect to the incorporation of Fe^{3+} into the structure of TiO_2 resulted band gap. The FTIR spectra shows a shift of peak at the wave number at 586 cm^{-1} and 774 cm^{-1} which is attribute of the Fe–O vibration as an indication of the formation of Fe-TiO_2 bonds. Incorporation of Fe^{3+} cation into the TiO_2 lattice replacing the Ti^{4+} ions, which induced a perturbation in anatase crystal structure, causes the change in the distance spacing of the crystal lattices d_{hkl} (101) of 8.9632 to 7.9413. The enhanced photocatalytic performance was observed for Fe-doped TiO_2/kaolinite compared with TiO_2/kaolinite with respect to *Escherichia coli* growth inhibition in solution media under visible light irradiation.

Keywords: Fe-doped TiO_2/kaolinite; photocatalyst; visible light; antibacterial; *Escherichia coli*

How to Cite: A.B. Aritonang, E. Pratiwi, W. Warsidah, S.I. Nurdiansyah, R. Risko (2021). Fe-doped TiO_2/Kaolinite as an Antibacterial Photocatalyst under Visible Light Irradiation. *Bulletin of Chemical Reaction Engineering & Catalysis*, 16(2), 293-301 (doi:10.9767/bcrec.16.2.10325.293-301)

Permalink/DOI: https://doi.org/10.9767/bcrec.16.2.10325.293-301

1. Introduction

The clean water is a primary need for living things, but its availability is increasingly limited. The quality of clean water tends to decline due to contamination of organic compounds and microorganism that can harm human health. The conventional technology used to treat water contaminated by the chlorination method. However, it is not environmentally friendly because produces residues of trihalomethane compounds in water which are carcinogenic [1]. Titanium dioxide (TiO_2) is a semiconductor material that, stable, non-toxic, has good photocatalytic activity, and has been widely used to degrade organic pollutants from water [2] and as an alternative disinfectant [3–4]. TiO_2 showed excellent antibacterial activities towards the fish bacteria pathogen, *Streptococcus iniae* and *Edwardsiella tarda* under UV light irradiation [5]. According to Ohtsu *et al.* [6], the TiO_2 have a strong oxidizing effect against unicellular organisms such as *Escherichia coli* bacteria. The strong oxidizing

*Corresponding Author.
Email: anthoni.b.aritonang@chemistry.untan.ac.id (A.B. Aritonang);
Telp: +62-0561-577963, Fax: +62-0561-577963

power of TiO_2 as photocatalyst can destroy prokaryotic bacterial cell membranes causing cytoplasmic leakage, which inhibiting bacterial metabolism and ultimately causing bacterial death by itself [7].

The TiO_2 absorbs photons energy in the UV region with wavelengths less than 380 nm and results a reactive oxygen species by reacting with water molecules and oxygen adsorbed in the surface of TiO_2 nanoparticles. However, the promising application has some limitations, due to the fact that the UV region occupies only approximately 4% of the full solar spectrum, because 45% of the energy belongs to the visible light, the remaining spectrum range belongs to infrared and longwave radiation [3].

Several attempts have been made to reduce the band gap of TiO_2 to make them visibly active using metal cation doping. One metal element that is suitable as a dopant is Fe^{3+} cation because it has an ionic radius of 0.064 nm, almost the Ti^{4+} ion (0.068 nm) will be substituted by Fe^{3+} ions in the TiO_2 structure [8]. According to Othman *et al.* [9], incorporation of Fe^{3+} ion into TiO_2 lattice caused shift the absorption peak from UV light to the visible light region, so it is more effectively used for the photocatalytic process in the environment.

In general, the TiO_2 nanoparticles are very susceptible to forming agglomerations to minimize their active surface area, so that their photocatalytic activity is reduced. On the other hand, it is difficult to separate the catalyst from the liquid medium for reuse. One of the possibilities to increase its photocatalytic activity is to introduce TiO_2 nanoparticles into the kaolinite. When the TiO_2 nanoparticles are immobilised into kaolinite, they still demonstrate photodegradable properties [10–12]. According to Dedkova *et al.* [10], the addition of kaolinite into TiO_2 composites increases the photocatalytic activity of inhibiting the growth of pathogenic bacteria. The kaolinite can also change acidobasic properties of the catalyst surface and prevent the formation of TiO_2 aggregates in suspension [11]. In addition, kaolinite can inhibit photo electron-photo hole pair recombination rate which contributes to increasing its photocatalytic activity [12,13]. Kaolinite capkala are natural clay minerals which are very abundant in Capkala village, Bengkayang region, including phylosilicates has an adsorption capacity of 0.65 mg/g, potentially used as a supporting material catalyst [14].

Many articles describing the fabrication of kaolinite/TiO_2 nanocomposites and perform a photocatalytic activity as an anti-bacterial has been published [10,15,16], wherever its photocatalytic activities as antibacterial were not clearly. Therefore, the aim of this study was to prepare and to characterize the Fe-doped TiO_2/kaolinite composite and evaluate its antibacterial activity for *Escherichia coli* under visible light irradiation.

2. Materials and Methods

2.1 Materials

Materials was used in this study are: Degussa P25, distilled water (H_2), titanium tetraisopropoxide (TTIP, Sigma-Aldrich 97%), ethanol (C_2H_5OH, Merck 96%), hydrochloric acid (HCl, Merck 98%), nitric acid 97% (HNO_3, Merck), glacial acetic acid (CH_3COOH, Merck 98%), acetylacetone (acac, Sigma-Aldrich 97%), ferric nitrate ($Fe(NO_3)_3$ (Sigma-Aldrich 97%), sodium chloride (NaCl, Sail brand 96%), kaolinite capkala (natural clay mineral from Capkala village, Bengkayang), *Escherichia coli* bacterial and yeast extract (Himedia).

2.2 Preparation of Kaolinite

Firstly, purification of kaolinite clay was performed by acid-base treatment as reported [10]. The kaolinite (1:1) are used in this research are kaolinite clay from Capkala village, Bengkayang Regency, West Kalimantan. Purification of kaolinite clay was carried out by acid-base method [14]. The initial kaolinite (5.0 gram) was mixed with 40 mL of 6 M HCl solution, followed activation process is carried out at 30 °C while stirring and left for 24 h. The solid was filtrated using a buchner funnel and washed with distilled water until it was free of Cl^- ions with the $AgNO_3$ test. The solid content separated from the dispersion was rinsed with distilled water and filtrated. Afterwards, the solid content was dried at 120 °C and kept for 60 min to remove the water bound and make surface active site of kaolinite and followed calcined at 500 °C for 2 h. Thus the obtained kaolinite were used for the further characterization and assessment.

2.3 Preparation of TiO_2 and Fe-doped TiO_2 Sol

The TiO_2 and Fe-doped TiO_2 nanoparticle was prepared by sol-gel method using titanium isopropoxide (TTIP) as titanium precursor. Preparation of Fe-doped-TiO_2 sol was carried out according to our previous report [17]. Briefly, 7.5 mL of TTIP and 26.5 mL of ethanol were mixed simultaneously into 2 mL acetic acid and 2 mL distilled water and put in a reflux

flask then added 1 mL acetylacetone. In order to produce sol the pure TiO_2, the dispersion was stirred at 55 °C for 3 h. The Fe-doped TiO_2 sol was prepared using the TiO_2 sol by adding Fe $(NO_3)_3$ solution with various concentrations of 0.05; 0.125; 0.25 (%w/v) until stirring for 2 h. The dispersion was left for 10 min to obtain Fe-doped TiO_2 sol. The TiO_2 and Fe-doped TiO_2 sol were immobilized to the kaolinite surface.

2.4 Preparation of Fe-doped TiO_2/Kaolinite

The 0.5 g of kaolinite was added in 10 mL distilled water and stirred for 15 min for uniform dispersion. Then, 25 mL Fe-doped TiO_2 sol which contained of Fe^{3+} (0.05; 0.125; 0.25 % w/v) was stirred together with the kaolinite dispersion for 4 h and followed aging for 12 h to form Fe-doped TiO_2/kaolinite gel. The Fe-doped TiO_2/kaolinite gel was rinsed with distilled water and dried at 80 °C for 4 h to form Fe-doped TiO_2/kaolinite solid. Afterwards, the solid content was calcined at 450 °C for 3 h to form Fe-doped TiO_2/kaolinite composite. Fe^{3+} cations doping, the TiO_2 crystal growth and anchored into the kaolinite surface have occurred simultaneously during calcination treatment [10,11,17]. The same procedure was carried out for TiO_2/kaolinite composite as a control. Thus, the composited obtained were used for the further characterization and photocatalytic activity test.

2.5 Characterization of Undoped and Fe-doped TiO_2/kaolinite Photocatalysts

Optical properties of the TiO_2/kaolinite and Fe-doped TiO_2/kaolinite were evaluated using UV-Visible diffuse reflectance spectrophotometry (DRS, Shimadzu 2450) with software UV Probe (DRS-8000 Shimadzu). Scans were performed over 200-800 nm and the band gap energy was determined using the tauch formula $(h\upsilon a)^{1/n} = A(h\upsilon - Eg)$. The various functional groups present in the samples were recorded with a FTIR analysis (Shimadzu IR Prastige-21) over a wavenumber range of 400–4000 cm^{-1}. The crystal structure of photocatalyst were determined using an X-ray diffractometer (XRD-Shimadzu-7000) which was operated at 40 KV and 30 mA with Cu-Kα 1 as radiation source of wavelength 1.54060 Å in the range scanning 20–80° (2θ). The average crystallite size of sample was calculate using Sherrer formula [19–21]: $D = k\,\lambda / (\beta \cos\theta)$, where $k = 0.94$; λ = 1.54060 Å; β full width half maximum (FWHM), and θ diffracting angle.

2.6 Antibacterial Test using Fe-doped TiO_2/ kaolinite as Photocatalyst

The antibacterial activity of the Fe-doped TiO_2 nanocomposite as photocatalyst under visible light irradiation was evaluated using the method described by Dedkova *et al.* [10] with several modification. Commercial nutrient agar for the cultivation bacteria were used. Liquid growth media were prepared and subsequently sterilized in an autoclave. Suspension of the Fe-doped TiO_2 photocatalyst in growth media was diluted to achieve concentrations of 5.0 mg/ml in the growth media which is contained of the bacterial inoculums of *Escherichia coli* an initial cell concentration of 1.3×10^9. The photocatalytic activity was evaluated in a tube reactor with a batch system equipped with a magnetic stirrer, equipped with a lamp Light Emitting Diode LED (50 W Watt BE-6205 LED flood light as visible light source, warm while and coolant to maintain the temperature in the reactor. The lamp was placed 10 cm above the reactor tube to induce photocatalytic reaction under visible light irradiation for 2 h. After the exposure living bacterial cells were determined according to visible growth inhibition.

The Optical Density (OD) method by UV-Visible spectrophotometer at a wavelength of 600 nm was carried out to determination of inhibition of against *Escherichia coli* [18,22,23]. The 0.125% Fe-doped TiO_2/kaolinite powder as photocatalyst was dispersed into sterile water for the *Escherichia coli* bacterial nursery model with a ratio of sterile water: bacteria (99:1). Absorbance measurements were carried out every 20 min at wavelength of 600 nm using a UV-Vis spectrophotometer (Shimadzu 2450). The reduction in turbidity was evaluated as an indication of the reduced quantity of *Escherichia coli* bacteria solution medium. The reaction solution (~2.0 mL) was quickly withdrawn at given reaction intervals and was returned to the reactor after being analyzed.

3. Results and Discussions

Synthesis of the Fe-doped TiO_2/kaolinite composite was carried out using the sol gel method because it can produce a material with high homogeneity [10,11]. Synthesis of TiO_2 was initiated by preparing TiO_2 sol using titanium tetra isopropoxide (TTIP) dissolved in ethanol and hydrolyzed by distilled water with the aid of acetic acid as catalyst. The TTIP precursors are very hygroscopic and easily react with water molecules, so it will be easier to

form large agglomerates or particles so that acetylacetone is added [2]. The hydrolysis stage occurs during the reflux process at 55 °C. The Fe-doped TiO_2 sol which has gone through the condensation and aging stages is heated using an oven at a temperature of ±80 °C to form Fe-doped TiO_2 amorphous. The Fe-doped TiO_2 amorphous is then calcined at 450 °C to form the crystal structure of Fe-doped TiO_2 [21]. During calcination process, both of the Ti^{4+} and Fe^{3+} cations compete with O atoms to form Fe–O–Ti bonding in the TiO_2 lattice and crystallite growth occurs simultaneously [3,21,24–26].

To study the optical properties of prepared photocatalysts, the UV-visible absorption spectra were recorded at room temperature and are shown in Figure 1(A). For the undoped TiO_2 exhibits absorption in a wavelength region below 380 nm is due to the intrinsic inter-band transition absorption of anatase TiO_2, while the absorption edge of Fe-doped TiO_2 is red shift toward visible light region. It indicates that the lattice defects and disorders introduced through the incorporation of the Fe^{3+} ions in TiO_2 lattice [27]. The band gap energy (Eg) of the photocatalysts was determined using Tauc equation [27–29].

$$(\alpha h\upsilon) = A(h\upsilon - Eg) \quad (1)$$

where α is the absorption coefficient, A is a constant depending on electronic transitions and $h\upsilon$ is the photon energy. The band gap energy (Eg) was obtained by taking the intercept of the extrapolation of the linear region of the plot $(\alpha h\upsilon)^2$ versus $h\upsilon$ (Figure 1(B)) and the calculation result are presented in the table in Figure 1(B) inset.

The band gap of the 0.05% Fe-doped TiO_2 (3.21 eV), and 0.25% Fe-doped TiO_2 (3.16 eV) decrease from 3.24 eV (TiO_2) is caused by incorporating Fe^{3+} ion to form Ti–O–Fe bonds [29]. These results suggest that 0.125% Fe-doped TiO_2 photocatalyst exhibit enhancement in photoresponse under visible light. This red shift which occurred for Fe-doped TiO_2 was evidenced by its corresponding into consideration the spin exchange interaction *sp-d* between band electrons and localized *d* electrons of Ti^{4+} ions substituting by the Fe^{3+} ions [29–30]. The band gap of the 0.125% Fe-doped TiO_2 is lower than all photocatalysts, so that the energy required to electron excite to the conduction band is easier and ultimately the photocatalyst activity will increase. However, according to Othman *et al.* [9], if the concentration of Fe^{3+} exceeds it will decrease its photocatalytic activity [7,9,24].

The Fourier transform infrared (FTIR) was carried out to investigate the vibration bands present in the prepared photocatalysts. The FTIR spectra of TiO_2 and Fe incorporated into TiO_2 lattice with 0.125 %wt. of the Fe^{3+} cation are presented in Figure 2. The vibration band can be defined in the range 500–4000 cm^{-1}. Figure 2 shows that the absorption peak occurs at a wave number between 3610–3786 cm^{-1} which is the stretching vibration of the OH group adsorbed onto the surface of the sample.

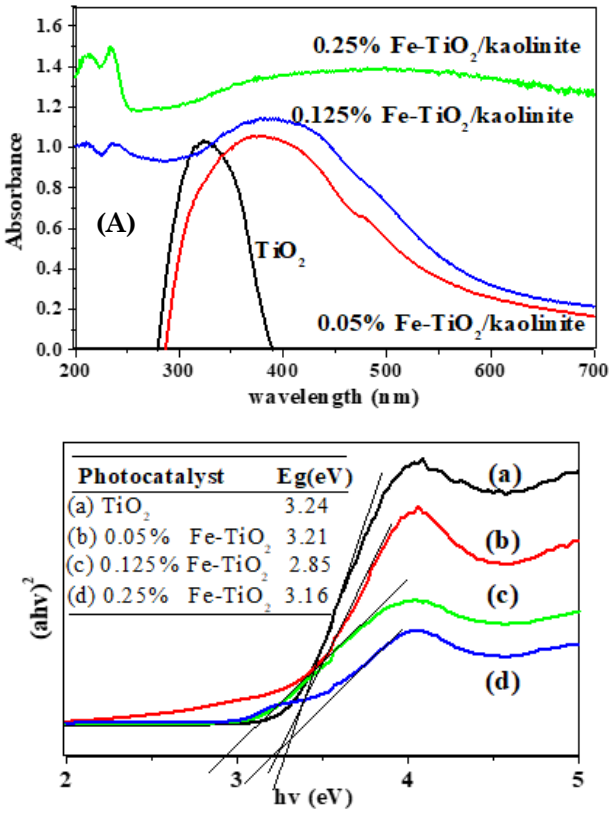

Figure 1. (A) UV-Vis absorbance spectra of TiO_2 and Fe-doped TiO_2. (B) Tauc plot.

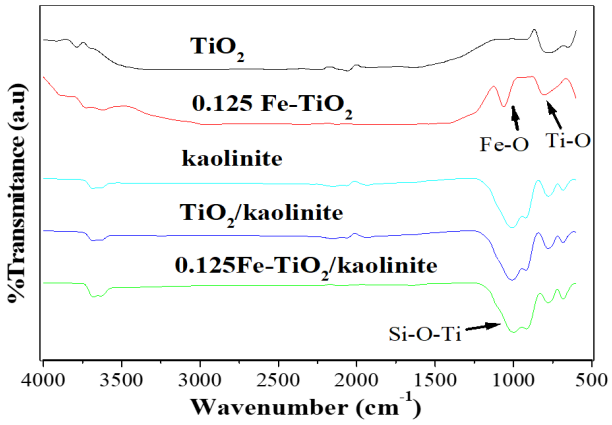

Figure 2. FTIR Spectra pattern for TiO_2/kaolinite and Fe-doped TiO_2/kaolinite.

The absorption peak at 602 cm^{-1} and 786 cm^{-1} observed on the spectrum of TiO_2 corresponded to the stretching vibrations of Ti–O–Ti [15,16,26,27]. It has been observed that the addition of Fe into TiO_2 matrix cause a shift of this band position to 586 cm^{-1} and 774 cm^{-1} for the Fe-doped TiO_2, it is considered as a sign of existence structure defect [27]. The band red shift was due to the formation of Fe–O bonds, which occurred following the substitution of Ti^{4+} with Fe^{3+} in the TiO_2 lattice. It is clearly observed on the spectra that incorporation of Fe^{3+} ion into TiO_2 matrix results in changes leading to the enhancement of absorption to a lower energy which consistent with UV-Vis spectra analysis.

The FTIR spectra of kaolinite showed the appearance of absorption peak at 3681 cm^{-1} which is characteristic of the O–H stretching vibration of H_2O adsorbed in kaolinite. The absorption peaks at 996 cm^{-1} and 600 cm^{-1} were characteristic of Al–O vibrations [31]. The vibration of Si–O–Si was shown the absorption peak at 695 cm^{-1} and 782 cm^{-1}. The absorption peak at 1000 cm^{-1} was the Si–O strain. FTIR spectra of TiO_2/kaolinite and Fe-TiO_2/kaolinite showed vibrations of Si–O–Ti at a wave number of 925 cm^{-1} [32]. However, the absorption peak of the Fe–O bond was not visible, because it was covered by the broad band of the Si–O–Ti vibration.

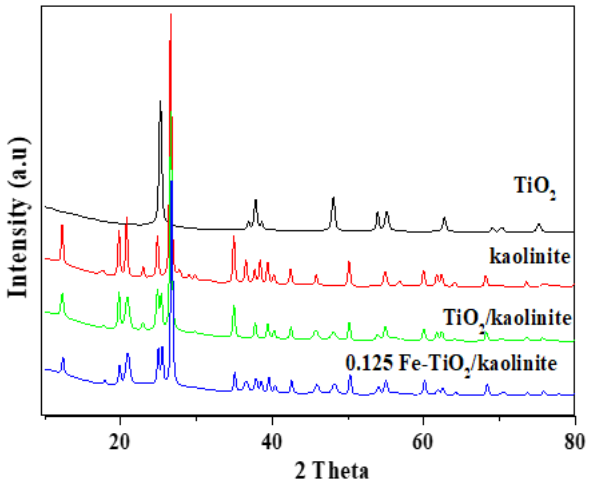

Figure 3. XRD pattern of TiO_2, Kaolinite and Fe-TiO_2/kaolinite.

The diffractogram patterns of TiO_2, kaolinite and Fe doped-TiO_2 are shown in Figure 3. The results of the calculation of crystallite size using the Debye-Scherrer (D) of Equation (2):

$$D = \frac{0.9\lambda}{\beta \cos\theta} \quad (2)$$

where, λ is the wavelength of the X-ray (1.54060 Å), β is the maximum peak half width (FWHM), θ is the diffraction angle (°). Figure 3 shows that there is a similarity between TiO_2 and Fe doped-TiO_2, which is in the range of 2θ 25°, 37°, and 48°. The three highest peaks indicate that TiO_2 has an anatase phase in accordance with JCPDS No. 01-075-8897. Signal from the 0.125% Fe-TiO_2 crystalline phase containing Fe of the doping elements could not be observed, which consistence with several articles [26,27]. However, a increase in the anatase peak intensity was observed for Fe-doped TiO_2, in comparison with TiO_2.

According to Mragui *et al.* [27], the Ti^{4+} ion was substituted by low-radius cations Fe^{3+} (0.65 Å) compared with Ti^{4+} (0.68 Å) causing a decrease in *d*-spacing and shifting band positions toward the high angle side [33]. Furthermore, incorporation of Fe^{3+} ion into the structures of TiO_2 and replaced the Ti^{4+} ions, which induced a perturbation in anatase crystal structure, causes crystal lattice distortion where it is shown that the change in the distance spacing of the crystal lattices d_{hkl} (101) is 8.9632 to 7.9413 and the peak position shifted. [21,34–37]. The crystallite size of TiO_2 was decreased (19.7711 nm) to 18.4733 nm as be seen in Table 1 indicated a slight shift to the higher angle side for Fe-doped TiO_2. According to the FTIR results, the formation of Fe-O bonds, which occurred following the substitution of Ti^{4+} with Fe^{3+} within the TiO_2 lattice causes a change in crystal size [35-37].

3.1 Photocatalytic Activity as Antibacterial *Escherichia coli*

Prior to photocatalytic reaction to inhibit the *Escherichia coli* growth PEC degradation,

Table 1. The peak (101) position.

Samples	Peak Position 2θ (°)	d_{hkl}	Crystallite size (nm)
TiO_2	25.2270	8.9632	19.7712
Kaolinite	24.8413	8.8768	-
TiO_2/Kaolinite	25.8444	9.9645	19.7711
0.125% Fe-TiO_2/Kaolinite	26.4773	7.8413	18.4733

the photocatalyst was dispersed into sterile water for the *Escherichia coli* bacterial nursery model in the dark for 1 h to establish the adsorption-desorption equilibrium [38]. During the photocatalytic process, the turbidity of solution which is a representation of *Escherichia coli* concentration was analyzed at a time interval of every 20 min by measuring the absorbance using a UV-visible spectrophotometer (Shimadzu 2450). The reaction solution (~2.0 mL) was quickly withdrawn at given reaction intervals and was returned to the reactor after being analyzed.

The effect of photocatalytic using TiO_2 and Fe-doped TiO_2/kaolinite composite as photocatalyst under visible irradiation for 2 h on the growth of *Escherichia coli* is shown in Figure 4a. We can see from that visible light (no catalyst) does not actively inhibit *Escherichia coli* growth. The *Escherichia coli* bacterial showed rapid growth, with the highest OD600 value being reached about 0.35 after visible light irradiated for 120 min. Generally, the TiO_2 photocatalyst is not active to absorb visible light, but in this work shows very low photocurrent (curve TiO_2), because the LED lamp as used as the visible light source contains UV light a portion of 10%. It can be seen in Figure 4a the TiO_2 have a low photocatalytic. After visible light irradiated for 120 min, the OD600 value of Fe-TiO_2/kaolinite is much lower than TiO_2/kaolinite and TiO_2, where arise to 0.01 and 0.23, respectively. It may be an indication that the formation of photogenerated electron-hole pairs on the surface of Fe-TiO_2/kaolinite is easier to occur than TiO_2 when absorbing visible light because it has a smaller band gap as a result of the mixing of the Fe 2p with Ti 2p orbitals [16–18]. These results are consistent with the absorption spectra. Obviously, the Fe^{3+} cation doping into TiO_2 lattice caused narrowed the band gap and improved the optical absorption visible light [20]. In contrast, the % inhibition for *Escherichia coli* value showed superior of Fe-TiO_2/kaolinite photocatalyst where is after visible irradiation for 120 min can growth inhibited the *Escherichia coli* 98% more higher than TiO_2/kaolinite and TiO_2 where arise 64.1 and 32.5, respectively. According to Dedkova *et al.* [10], the lower activity antibacterial of the kaolinite/TiO_2 is caused by the lower production of reactive oxygen species antibacterial activity of (ROS).

Surface properties of the composites are changing during the calcination process, which could lead to increase of ROS production. The kaolinite is exposed to the temperatures higher than approximate 470 °C and it starts to lose its interlayer water and dehydroxylation of the kaolinite structure occurs [17]. There was improved the surface area of the photocatalyst caused enhance its capacity absorption. Electron/hole pairs are generated if TiO_2 interacts with light with an energy which is larger than the TiO_2 band gap. The generated electron/hole pair can react with O_2 and H_2O when superoxide anion radicals ($O^{2-}\bullet$) and hydroxyl radicals ($\bullet OH$) are formed. These oxidative species are highly reactive, which could be the major reason of antimicrobial activity of titanium dioxide [11], and thus the amount of produced ROS is important [12,13]. Another factor which must be taken into account is the viability of microorganisms, ability of a cell to divide itself in a short time and growth according to particular growth curve [16]. It was clearly that the higher growth inhibition of *Escherichia coli* are simultaneously contribution of the high surface area of kaolinite as site active to substrate absorption [11–13]. Another factor of the superox-

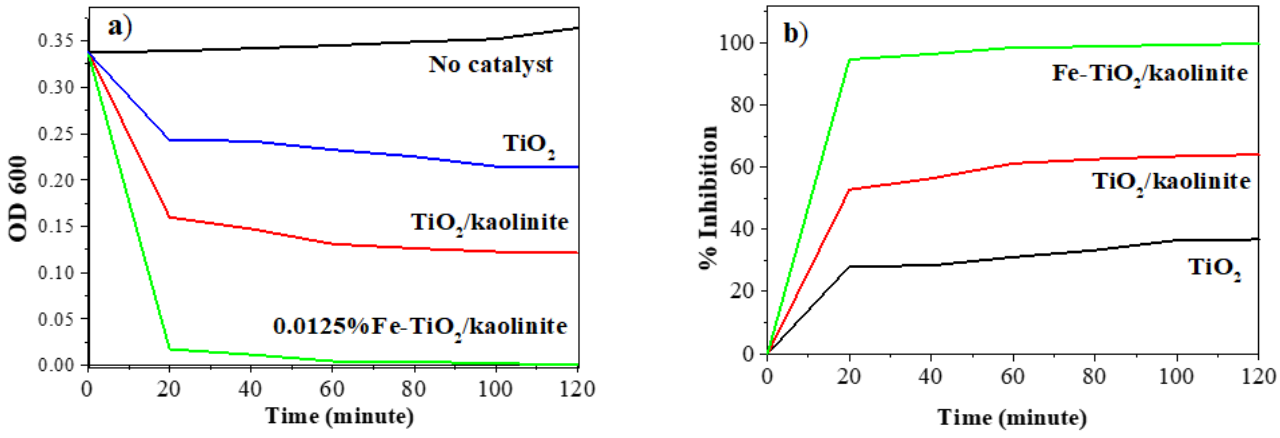

Figure 4. Growth curves treated: a) Photocatalytic under Visible Irradiation, b) % Inhibition for *Escherichia coli*.

ide anion radicals ($O^{2-}\bullet$) and hydroxyl radicals ($\bullet OH$) pairs are able to oxidize bacteria [22,23].

4. Conclusions

The Fe-doped TiO_2 photocatalysts with an atomic ratio of (0.125%) Fe:TiO_2 immobilized on kaolinite surface have been produced. The band gap of the Fe-doped TiO_2 (2.85 eV) decrease from 3.24 eV (TiO_2) was caused by incorporating Fe^{3+} ion to form Ti−O−Fe bonds. These results suggest that 0.125% Fe-doped TiO_2 photocatalyst exhibit enhancement in photoresponse under visible light. Incorporation of Fe^{3+} cation into the TiO_2 lattice and replaced the Ti^{4+} ions, which induced a perturbation in anatase crystal structure, causes crystal lattice distortion where it is shown that the change in the distance spacing of the crystal lattices d_{hkl} (101) is 8.9632 to 7.9413 and the peak position shifted. The Fe-TiO_2/kaolinite photocatalyst shows superior photocatalytic activity after visible irradiation for 120 min can growth inhibited the *Escherichia coli* 98% more higher than TiO_2/kaolinite and TiO_2 where arise 64.1 and 32.5, respectively.

Acknowledgments

This work was supported by DIPA grand 2020, Faculty of Mathematics and Natural Science, Tanjungpura University.

References

[1] Ma, S., Zhan, S., Jia, Y., Zhou, Q. (2015). Superior antibacterial activity of Fe_3O_4-TiO_2 nano sheets under solar light. *ACS Applied Materials & Interfaces*, 7(39), 21875–21883. DOI: 10.1021/acsami.5b06264.

[2] Tsiampalis, A., Mantzavinos, D., Frontistis, Z., Binas, V., Kiriakidis, G. (2019). Degradation of sulfamethoxazole using iron-doped titania and simulated solar radiation. *Catalysts*, 9, 612. DOI: 10.3390/catal9070612.

[3] Haghi, M., Hekmatafshar, M., Janipour, M.B., Gholizadeh, S.S., Faraz, M.K., Sayyadifar, F., Ghaedi, M. (2012). Antibacterial effect of TiO_2 nanoparticles on pathogenic strain of E. coli. *International Journal of Advanced Biotechnology and Research*, 3(3), 621–624.

[4] Li, Q., Mahendra, S., Lyon, D.Y., Brunet, L., Liga, M.V., Li, D., Alvarez, P.J.J. (2008). Antimicrobial nanomaterials for water disinfection and microbial control: potential applications and implications. *Water Research*, (42), 4591–4602. DOI:10.1016/j.watres.2008.08.015

[5] Cheng, T.C., Chang, C.Y., Chang, C.I., Hwang, C.J., Hsu, H.C., Wang, D.Y., Yao, K.S. (2008). Photocatalytic bactericidal effect of TiO_2 film on fish pathogens. *Surface and Coatings Technology*, 203(5–7), 925–927. DOI: 10.1016/j.surfcoat.2008.08.022.

[6] Ohtsu, N., Yokoi, K., Saito, A. (2015). Fabrication of Visible-Light-Responsive Photocatalytic Antibacterial Coating on Titanium through Anodic Oxidation in a Nitrate/Ethylene Glycol Electrolyte. *Surface and Coatings Technology*, 261, 97–102. DOI: 10.1016/j.surfcoat.2014.12.021.

[7] Vymětalová, V., Remsa, J., Jelínek, M., Písařík, P., Mikšovský, J., Řasová, V. (2016). Antibacterial activity of Titanium dioxide and Ag-incorporated DLC thin film. *Lékař a technika*, 46(3), 65–68.

[8] Marami, M., Farahmandjou, M., Khoshnevisan, K. (2018). Sol-Gel Synthesis of Fe-doped TiO_2 Nanocrystals. *Journal of Electronic Materials,* 47(7), 1–8. DOI: 10.1007/s11664-018-6234-5

[9] Othman, S.H., Rashid, S.A., Ghazi, T.I.M., Abdullah, N. (2011). Fe-doped TiO_2 nanoparticles produced via MOCVD: synthesis, characterization, and photocatalytic activity. *Journal of Nanomaterials*, 2011, 571601. DOI: 10.1155/2011/571601.

[10] Dedkova, K., Matejova, K., Lang, J., Peikertova, P., Kutlakova, K.M., Neuwirthova, L., Frydrysek, K., Kukutschova, J. (2014). Antibacterial activity of kaolinite/nano TiO_2 composites in relation to irradiation time. *Journal of Photochemistry and Photobiology B: Biology*, 135, 17–22. DOI: 10.1016/j.jphotobiol.2014.04.004.

[11] Koci, K., Matejka, V., Kovar, P., Lacny, Z., Obalova, L. (2011). Comparison of the pure TiO_2 and kaolinite/TiO_2 composite as catalyst for CO_2 photocatalytic reduction. *Catalysis Today*, 161, 105–109. DOI: 10.1016/j.cattod.2010.08.026.

[12] Li, X., Peng, K., Chen, H., Wang, Z. (2018). TiO_2 nanoparticles assembled on kaolinites with different morphologies for efficient photocatalytic performance. *Scientific Reports*, 8, 11663–11673. DOI: 10.1038/s41598-018-29563-8.

[13] Mora, L.D., Nassar, E.J., Bonfirm, L.F., Barbosa, L.V., da Silva, T.H., Trujillano, R., Ciuffi, J.K., González, B., Vicente, M.A., Gil, A., Rives, V., Perez-Bernal, M.E., Korili, S., Faria, E.H. (2019). White and red Brazilian São Simão's kaolinite-TiO_2 nanocomposites as catalysts for toluene from aqueous solutions. *Materials*, 12(23), 3943. DOI: 10.3390/ma12233943.

[14] Listiani, D., Safar, A., Aritonang, A.B. (2019). Sintesis TiO_2-kaolin dan uji aktivitas fotokatalisis untuk antibakteri staphylococcus aureus dan escherichia coli. *Indonesia Journal Pure Application Chemistry*, 2(3), 130–139.

[15] Arshad, M., Qayum, A., Muhammad, S.J. (2018). Assessment of antioxidant and antibacterial activities of iron-titanium oxide nanoparticles synthesized in various solvents and their microscopic characterization. *Pakistan Journal of Science*, 70(2), 113–118.

[16] Meng, D., Liu, X., Xie, Y., Du, Y., Yang, Y., Xiao, C. (2019). Antibacterial activity of visible light-activated TiO_2 thin films with low level of Fe doping. *Advances in Materials Science and Engineering*, 2019, 5819805. DOI: 10.1155/2019/5819805.

[17] Pratiwi, E., Harlia, H., Aritonang, A.B. (2020). Sintesis TiO_2 terdoping Fe^{3+} untuk degradasi rhodamin B secara fotokatalisis dengan bantuan sinar tampak. *Positron*, 10(1), 57–63. DOI: 10.26418/positron.v10i1.37739.

[18] Huang, W., Wang, J.Q., Song, H.Y., Zhang, Q., Liu, G.F. 2017. Chemical analysis and in vitro antimicrobial effects and mechanism of action of Trachyspermum copticum essential oil against Escherichia coli. *Asian Pasific Journal of Tropical Medicine*, 10(7), 663–669. DOI: 10.1016/j.apjtm.2017.07.006.

[19] Al-Jawad, S.M.H., Taha, A.A., Salim, M.M., (2017). Synthesis and characterization of pure and Fe doped TiO_2 thin films for antimicrobial activity. *Optik*, 142, 42–53. DOI: 10.1016/j.ijleo.2017.05.048.

[20] Ghorbanpour, M., Feizi, A. (2019). Iron-doped TiO_2 Catalysts with Photocatalytic Activity. *Journal of Water and Environmental Nanotechnology*, 4(1), 60–66.

[21] Nasralla, N., Kompany, A., Yeganeh, M., Astut,i Y., Piticharoenphun, S., Shahtahmasebi, N., Karimipour, M., Mendis, B.G., Poolton, N.R.J., Šiller L. (2013). Structural and spectroscopic study of Fe-doped TiO_2 nanoparticles prepared by sol-gel method. *Scientia Iranica*, 20(3), 1018–1022. DOI: 10.1016/j.scient.2013.05.017.

[22] Lucidi, M., Marsan, M., Pudda, F., Frangipani, E., Visca, P. (2019). Geometrical-optics approach to measure the optical density of bacterial cultures using a LED-based photometer. *Biomedical Optics Express*, 10(11), 5600–5610. DOI: 10.1364/BOE.10.005600.

[23] Begot, C., Desnier, I., Daudin, J.D., Labadie, J.C., Lebert, A. (1996). Recommendations for calculating growth parameters by optical density measurements. *Journal of Microbiological Methods*, 25, 225–232. DOI: 10.1016/0167-7012(95)00090-9.

[24] Stoyanova, A.M., Hitkova, H.Y., Ivanova, N.K., Bachvarova-Nedelcheva, A.D., Iordanova, R.S., Sredkova, M.P. (2013). Photocatalytic and antibacterial activity of Fe-doped TiO_2 nanoparticles prepared by nonhydrolytic sol-gel method. *Bulgarian Chemical Communications,* 45(4), 497–504.

[25] Kiwi, J., Rtimi, S. (2018). Mechanisms of the Antibacterial Effects of TiO_2-FeOx under Solar or Visible Light: Schottky Barriers versus Surface Plasmon Resonance. *Coatings*, 8(11), 391. DOI: 10.3390/coatings8110391.

[26] Werapun, U., Pechwang, J. (2019). Synthesis and antimicrobial activity of Fe:TiO_2 particles. *Journal of Nano Research*, 56, 28–38. DOI:10.4028/www.scientific.net/JNanoR.56.28.

[27] Mragui, A.E., Logvina, Y., da Silva, L.P., Zegaoui, O., Esteves da Silva, J.C.G. (2019). Synthesis of Fe- and Co-doped TiO_2 with improved photocatalytic activity under visible irradiation toward carbamazepine degradation. *Materials,* 12(23), 3874. DOI: 10.3390/ma12233874.

[28] Khan, M.A.M., Siwach, R., Kumar, S., Alhazaa, A.N. 2019. Role of Fe doping in tuning photocatalytic and photoelectrochemical properties of TiO_2 for photodegradation of methylene blue, *Optics and Laser Technology*, 118, 170-178.

[29] Khan, M.A.M., Kumar, S., Alhazaa, A.N., Al-Gawati, M.A. (2018). Modifications in structural, morphological, optical and photocatalytic properties of ZnO: Mn nanoparticles by sol-gel protocol. *Materials Science in Semiconductor Processing*, 87, 134–141. DOI: 10.1016/j.mssp.2018.07.016.

[30] Channei, D., Inceesungvorn, B., Wetchakun, N., Ukritnukun, S., Nattestad, A., Cen, J., Phanichphant, S. (2014). Photocatalytic degradation of methyl orange by CeO_2 and Fe-doped CeO_2 films under visible light irradiation. *Scientific Reports*, 4, 5757. DOI: 10.1038/srep05757.

[31] Hosseini, S.A., Niaei, A., Salari, D. (2011). Production of Al_2O_3 from Kaolin. *Open Journal of Physical Chemistry,* 1(2), 23–27. DOI: 10.4236/ojpc.2011.12004.

[32] Kutlakova, K.M., Tokarsky, J., Kovar, P., Vojteskovaa, S., Kovarova, A., Smetana, B., Kukutschova, J., Capkova, P., Matejka, V. (2011). Preparation and Characterization of Photoactive Composite Kaolinite/TiO_2. *Journal of Hazardous Materials*, 188(1-3), 212–220. DOI: 10.1016/j.jhazmat.2011.01.106.

[33] Lin, C.Y.W., Channei, D., Koshy, P., Nakaruk, A., Sorrell, C.C. (2012). Effect of Fe doping on TiO_2 films prepared by spin coating. *Ceramics International*, 38, 3943-3946, doi:10.1016/j.ceramint.2012.01.047

[34] Adyani, S.M., Ghorbani, M.A. (2018). A comparative study of physicochemical and photocatalytic properties of visible light responsive Fe, Gd and P single and tri-doped TiO2 nanomaterials. *Journal of Rare Earths*, 36(1), 72–85. DOI: 10.1016/j.jre.2017.06.012.

[35] Zhu, J., Chen, F., Zhang, J., Chen, H., Anpo, M. (2006). Fe^{3+}-TiO_2 photocatalysts prepared by combining sol-gel method with hydrothermal treatment and their characterization. *Journal of Photochemistry and Photobiology A: Chemistry*, 180(1-2), 196–204. DOI: 10.1016/j.jphotochem.2005.10.017.

[36] Komaraiah, D., Radha, E., Kalarikkal, N., Sivakumar, J., Ramana R., M.V., Sayanna, R. (2019). Structural, optical and photoluminescence studies of sol-gel synthesized pure and iron doped TiO_2 photocatalysts. *Ceramics International*, 45(18B), 25060–25068. DOI: 10.1016/j.ceramint.2019.03.170.

[37] Khan, M., Cao, W. (2013). Cationic (V, Y)-codoped TiO_2 with enhanced visible light induced photocatalytic activity: A combined experimental and theoretical study. *Journal of Applied Physics,* 114, 183514. DOI: 10.1063/1.4831658.

[38] Heller, A.A., Spence, D.M. (2018). A rapid method for post-antibiotic bacterial susceptibility testing. *PLoS ONE,* 14(1), e0210534. DOI: 10.1371/journal.pone.0210534.

Selected and Revised Papers from 3rd International Conference on Chemistry, Chemical Process and Engineering 2020 (IC3PE 2020) (https://chemistry.uii.ac.id/ic3pe/) (Universitas Islam Indonesia (UII), Labuan Bajo, Nusa Tenggara Timur, Indonesia by 30th September – 1st October 2020) after Peer-reviewed by Scientific Committee of IC3PE 2020 and Peer-Reviewers of Bulletin of Chemical Reaction Engineering & Catalysis. Editors: Is Fatimah, I. Istadi